JTTEE5 17:360–364
DOI: 10.1007/s11666-008-9185-1
1059-9630/$19.00 © ASM International

Production and Characterization of Metastable ZrO_2-Al_2O_3Coatings Obtained by APS + Quench

S. Dosta, I.G. Cano, J.R. Miguel, and J.M. Guilemany

(Submitted July 30, 2007; in revised form January 14, 2008)

Producing nanostructured materials through metastable phases is an interesting novel route in the field of ceramic materials. Due to their small grain size and uniform structure, these nanostructured bulk materials exhibit very interesting properties. Metastable coatings can be produced starting from microstructured powders through atmospheric plasma spray technique, followed by a quenching route. The initial powders are melted during the spraying and deposited over a substrate that is quenched with liquid nitrogen feeders, producing metastable coatings. The thermal-sprayed coatings have been characterized using x-ray diffraction, scanning electron microscopy, field emission scanning electron microscopy, and energy dispersive spectroscopy. The properties of such coatings have been also studied obtaining promising results.

Keywords APS coatings, ceramic oxide layers, manufacturing, nanostructured coatings, nanostructured materials, processing, properties, thermal and phase stability of coatings

1. Introduction

Recent research (Ref 1, 2) in the field of nanostructured ceramic materials has underscored the importance of using feedstock powders with metastable phases. Grain growth is reduced due to the immiscibility of the two phases in the solid state, and the obtained materials exhibit very interesting properties such as higher hardness and toughness (Ref 3).

Plasma-sprayed ZrO_2 coatings have been used as thermal protection for aircraft engines parts such as combustor cans, nozzle and walls, or gas path transition pieces. Moreover, the hardness of ZrO_2 coatings can be improved with the addition of Al_2O_3. In this study, ZrO_2-Al_2O_3 system has been selected to study how nanostructured coating can be obtained by atmospheric plasma spray (APS) technology following a metastability route.

To obtain nanostructured coatings, one way is to use nano-scaled agglomerated powders but, these feedstock powders are usually very expensive and it is difficult to preserve the nano-scale during the high-temperature process.

Another way consists of obtaining nanostructured coatings through metastable states. These metastable states can be obtained by APS followed of a cooling process.

During a conventional APS process, the initial powder is melted for its residence in the hot zone of the plasma jet and then the molten particles are deposited over a substrate producing a coating. This results in a combination of phases where metastable and equilibrium phases coexist. Previous researches (Ref 4-6) described the use of thermal spray to obtain coatings which were formed by metastable phases due to the high-thermal gradient involved in the spraying process. Actually these ''metastable'' coatings are also composed of stable phases (equilibrium phases) while as a totally metastable state can be achieved with an ultrahigh cooling rate (Ref 7, 8). When a heat treatment of the totally metastable coatings is carried out, the existing phases transform to the equilibrium ones producing nanostructured free-standing coatings. It is due to the mutually suppression of grain growth as a direct consequence of the immiscibility of the phases in the solid state.

In this work, ZrO_2-Al_2O_3 coatings were produced by APS attaining a totally metastable state through a quench process. This process used liquid nitrogen supplied by feeders in continuous flow, achieving coatings with thickness of 250 μm formed by only metastable phases.

The obtained coatings were characterized using x-ray diffraction (XRD), scanning electron microscopy (SEM), field emission scanning electron microscopy (FESEM), and energy dispersive spectroscopy (EDS). Hardness was analyzed by indentation method and the result showed improvements in relation with the conventional coatings.

2. Experimental Procedure

A commercially available ZrO_2-20 wt.% Al_2O_3 powder has been used as feedstock in the present study

S. Dosta, I.G. Cano, J.R. Miguel, and **J.M. Guilemany**, Thermal Spray Centre (CPT), Department of Ciència dels Materials i Enginyeria Metal·lúrgica, Universitat de Barcelona, Barcelona, Spain. Contact e-mail: sdosta@ub.edu.

(Tosoh, Japan). This powder contains an addition of 3 mol% Y_2O_3 to stabilize the tetragonal zirconia phase (t-ZrO_2) and it is an agglomerated and sintered powder. The mean particle size of this powder is 57 μm.

To obtain metastable phases, the ZrO_2-Al_2O_3 powder has been sprayed using an F4 plasma torch and refrigerated layer by layer with two liquid nitrogen feeders (Air Products, S.A.). They were sprayed over a steel 50 mm × 20 mm × 5 mm flat substrate (UNS G41350). The substrates were previously degreased with acetone and grit blasted with corundum at 5.6 bar, 45° using a blasting distance of 250 mm. The grit-blasted substrates had a mean roughness (Ra) of about 5 μm, being always higher than 4 μm.

The characterization of the samples included SEM-FESEM images and EDS phase analysis. More accurate phase analysis of the starting powders and coatings was performed by XRD.

Cross-sectional microhardness measurements were performed by means of Vickers indentation at 300 gf load, and the indentations were measured with an optical microscope to increase measurement accuracy.

3. Results and Discussion

3.1 Feedstock Powder

Figure 1a shows the free-surface micrographs of the initial powder. This powder exhibits a spherical morphology and fine particles of Al_2O_3 are homogeneously distributed over the ZrO_2 matrix as can be seen in the cross-sectional BSE-SEM image (Fig. 1b) where the brighter particles correspond to Al_2O_3.

The XRD spectrum is shown in Fig. 2, where the main phase is t-ZrO_2. A small amount of monoclinic ZrO_2, formed due to the partially stabilization with yttria is also observed. The XRD pattern also shows peaks corresponding to α-Al_2O_3 phase, that is the equilibrium phase at room temperature.

3.2 Coatings

SEM cross-sectional images of the as-sprayed ZrO_2-Al_2O_3 coatings (using the APS + quenching route) are shown in Fig. 3. It can be observed a homogeneous structure with a thickness around 250 μm. The porosity has been estimated in 15% being a typical value for a coating obtained by APS. Nondifferentiated phases are observed in Fig. 3 as can be corroborated by the XRD pattern (Fig. 3b), that shows no presence of Al_2O_3. Just a mixture of cubic and tetragonal ZrO_2 phase have been identified. The main phase is the cubic phase, being a significant result because it is a nonequilibrium phase at room temperature. The fact that Al_2O_3 phase is not detected in the XRD pattern could be explained by the formation of amorphous Al_2O_3 or/and some dissolution in the ZrO_2 matrix. The high-cooling rate used in the process can lead to the integration of aluminum in the cubic zirconia cell. When the indexation of the peak corresponding to cubic phase is done, the lattice parameter ($d \approx 4.93$) result is smaller than the standard pattern. This is coherent due to the smaller radius of Al^{3+} (0.068 nm) than Zr^{4+} (0.086 nm). Rietveld refinement is being carried out to determinate this mechanism.

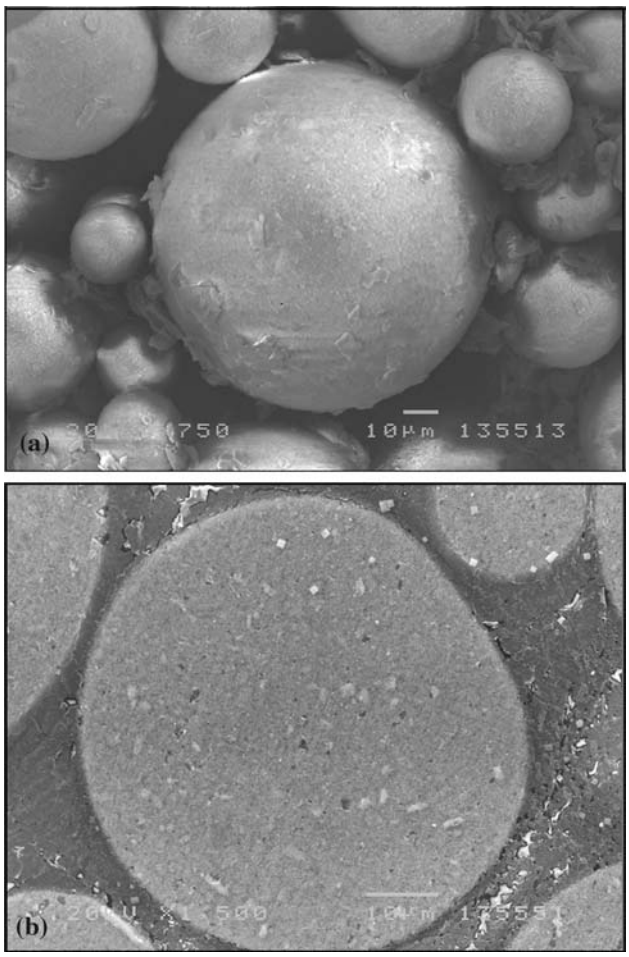

Fig. 1 SEM (a) free-surface and (b) cross-sectional images of ZrO_2-Al_2O_3 feedstock powder where the brighter particles correspond to Al_2O_3

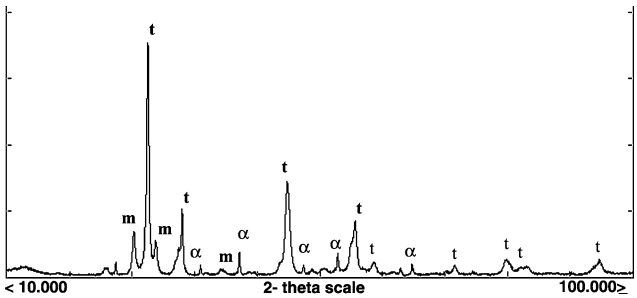

Fig. 2 XRD pattern of ZrO_2-20 wt.% Al_2O_3 feedstock powder

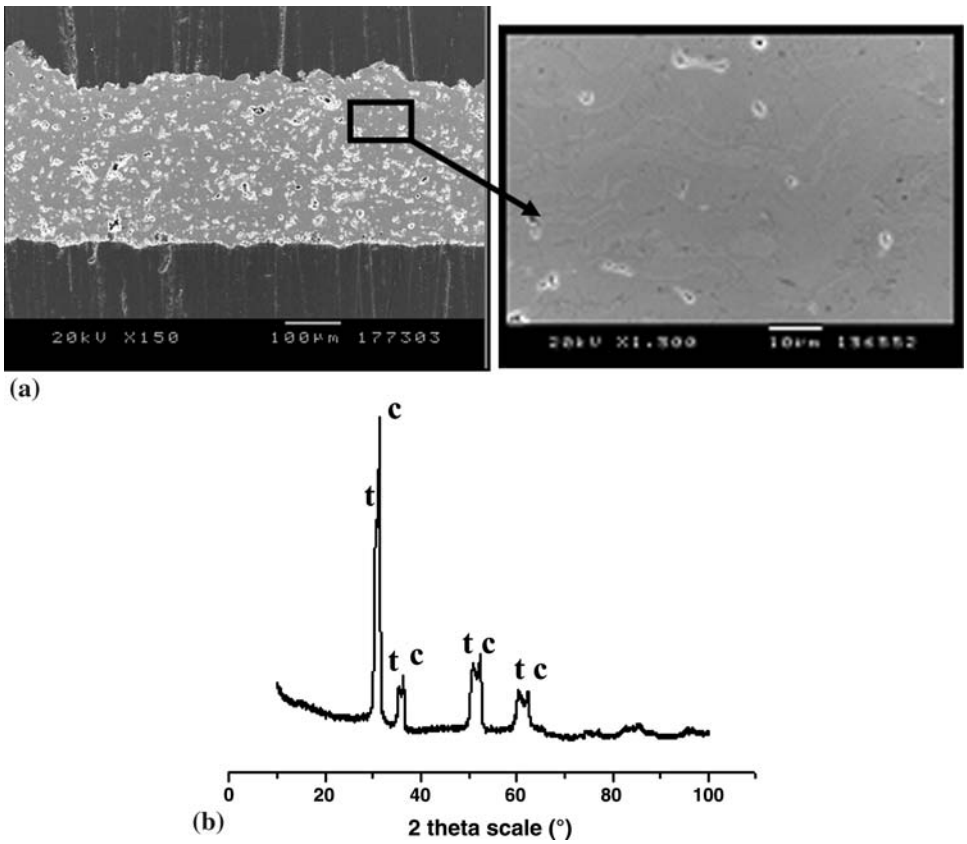

Fig. 3 As-sprayed ZrO_2-20 wt.% Al_2O_3 coating (a) cross-sectional image and (b) XRD, where *t* means ZrO_2-tetragonal phase and *c* means ZrO_2-cubic phase of ZrO_2-20 wt.% Al_2O_3 as-sprayed coating

The as-sprayed coatings were heat treated at 1200 and 1400 °C for 1 h and the resulting materials were characterized by XRD and SEM. After the thermal treatment carried out at 1200 °C, the XRD spectrum only showed the presence of ZrO_2 (tetragonal) phase, which is predicted by the equilibrium phase diagram when the ZrO_2 is doped with Y_2O_3. No presence of Al_2O_3 was detected as Fig. 4 shows although Al_2O_3 precipitates are observed. This can be attributed to be in the first stages of the precipitation phenomena because after the thermal treatment at 1400 °C, α-Al_2O_3 equilibrium phase clearly appears (Fig. 5b). Al_2O_3 grains have kept their nanometric size even at 1400 °C as can be seen in Fig. 6, where a TEM image shows the nanometric precipitates of Al_2O_3 into a ZrO_2 matrix.

3.3 Microhardness Values

Representative Vickers microhardness values ($HVN_{300\ gf}$) obtained for the as-sprayed ZrO_2-20 wt.% Al_2O_3 coating have been $HVN_{300\ gf} = 649 \pm 80$.

Once heat treated at 1200 °C was carried out, the nucleation of α-Al_2O_3 and the reduction of the porosity were achieved in the ZrO_2-Al_2O_3 coatings. Thus, the microhardness value increased being $HVN_{300\ gf} = 1063 \pm 86$ for the coating heat-treated at 1200 °C (Fig. 7).

Image analysis (Software Matrox Inspector v. 1.71) was used to quantify coatings porosity. Quoted values are an average of 10 areas at the same magnification for each coating. Porosity measured by image analysis was 16.8% ± 0.3 for the metastable coating, being 15.5% ± 0.5 and 11.3% ± 0.4 for the heat-treated coatings at 1200 and 1400 °C, respectively. The pores are randomly scattered throughout the cross section and has been reduced as the treatment temperature increased.

After the heat treatment at 1400 °C, a little grain growth is produced for the Al_2O_3 phase and porosity is also reduced. $HVN_{300\ gf}$ obtained for the coating heat treated at 1400 °C were $HVN_{300\ gf} = 1219 \pm 36$, which means that the microhardness value was doubled when compared to the as-sprayed coating. Microhardness has increased due to the reduction of porosity, but also for the full precipitation of Al_2O_3. In the XRD pattern of samples treated at 1200 °C, only ZrO_2 is detected due to the noncomplete precipitation of Al_2O_3. When the total Al_2O_3 has precipitated in form of nanograins, the state of maximum hardness is achieved due to the reinforcement mechanisms.

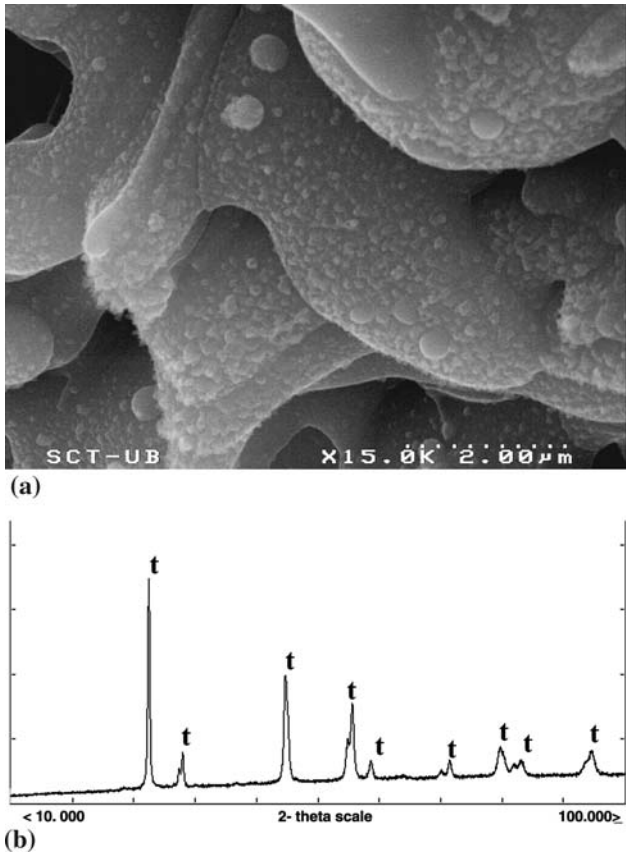

Fig. 4 (a) Free-surface images and (b) XRD where *t* means ZrO_2-tetragonal phase of the of ZrO_2-20 wt.% Al_2O_3 coating treated at 1200 °C for 1 h

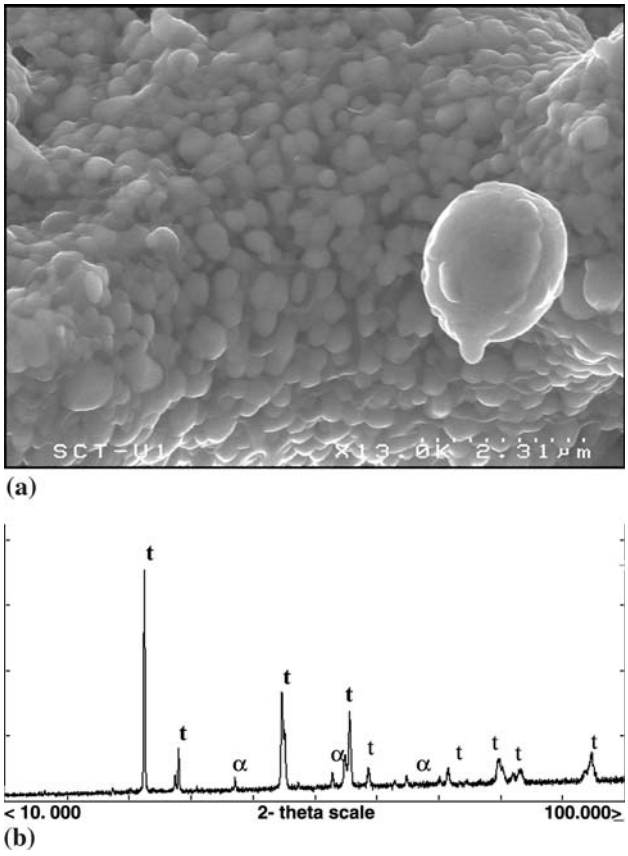

Fig. 5 (a) Free-surface images and (b) XRD where *t* means ZrO_2-tetragonal phase of the ZrO_2-20 wt.% Al_2O_3 coating treated at 1400 °C for 1 h

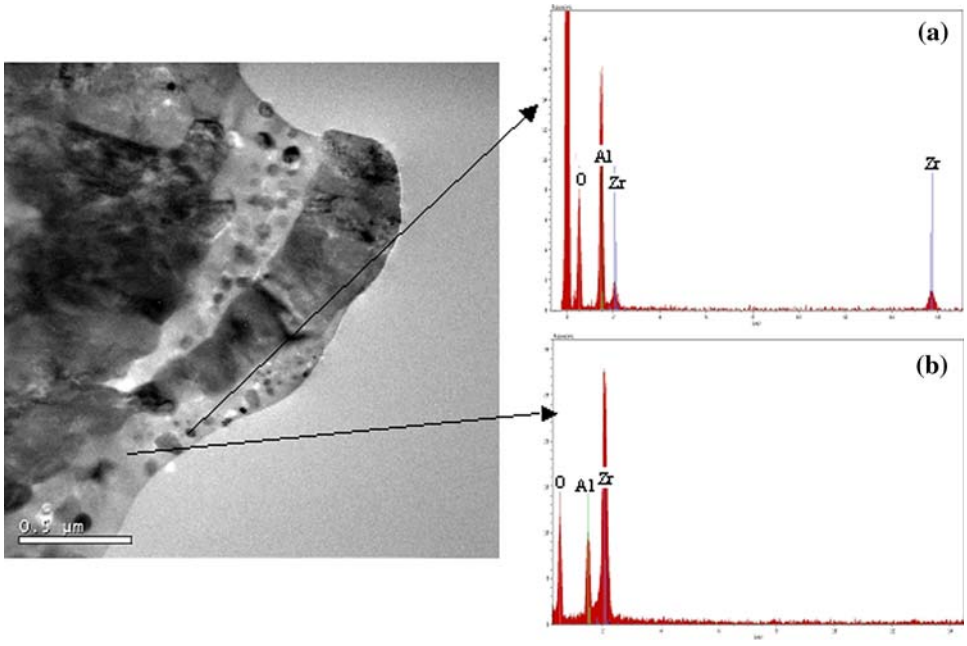

Fig. 6 TEM image of ZrO_2-20 wt.% Al_2O_3 heat-treated at 1400 °C with EDS analysis corresponding to the nanometric precipitates of Al_2O_3 (a) into a ZrO_2 matrix (b)

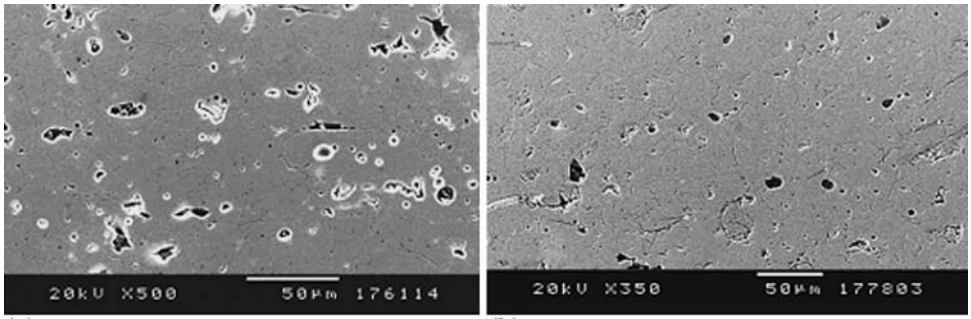

Fig. 7 Cross-sectional images of ZrO_2-20 wt.% Al_2O_3 heat-treated at (a) 1200 °C and (b) 1400 °C

4. Conclusions

- ZrO_2-20 wt.% Al_2O_3 system has been tested to obtain metastable coatings by atmospheric plasma spraying technology followed of a quenching process.
- As-sprayed coatings exhibited microstructural homogeneity and were composed by a combination of tetragonal and cubic ZrO_2 phases.
- These metastable structures evolved to equilibrium phases after the heat-treatments. Final structures were formed by nanometric grains.
- After the heat-treatments, microhardness values were improved (80%) in relation to values of conventional coatings. This improvement was attributed to the reduction of porosity and the precipitation of Al_2O_3

Acknowledgments

The authors wish to thank the University of Barcelona for the financial support for this research, to the UE for the project NAMAMET STRP-001470, to the Generalitat de Catalunya for the project 2005 SGR-00310 and to the Ministerio de Educación y Ciencia for the project MAT2007-65179.

References

1. G.S. Walker, E. Williams, and A.K. Bhattacharya, Preparation and Characterization of High Surface Area Alumina-Titania Solid Acids, *J. Mater. Sci.*, 1997, **32**, p 5583-5592
2. V. Viswanathan, T. Laha, K. Balani, A. Agarwal, and S. Sea, Challenges and Advances in Nanocomposite Processing Techniques, *Mater. Sci. Eng. R*, 2006, **54**, p 121-285
3. S.A. Jansen, S.A. Grabatia, and N.M. Buecheler, Electronic Properties of Alumina/Titania Mixed Oxides and Interfacial Surface Models: A Theoretical Analysis, *Mater. Res. Soc. Symp. Proc.*, 1993, **291**, p 227-232
4. N.N. Ault, Characteristics of Refractory Oxide Coating Produced by Flame-Spraying, *J. Amer. Ceram. Soc.*, 1957, **40**, p 69-74
5. R. McPherson, On the Formation of Thermally Sprayed Alumina Coatings, *J. Mater. Sci.*, 1980, **15**, p 3141-3149
6. A. Agarwal, T. McKechnie, and S. Seal, Net Shape Nanostructured Aluminum Oxide Structures Fabricated by Plasma Spray Forming, *J. Therm. Spray. Technol.*, 2003, **12**, p 350
7. B.H. Kear, J. Colaizzi, W.E. Mayo, and S.C. Liao, On the Processing of Nanocrystalline and Nanocomposite Ceramics, *Scripta Mater.*, 2001, **44**(8/9), p 2065-2068
8. I.G. Cano, S. Dosta, J.R. Miguel, and J.M Guilemany, Production and Characterization of Metastable Al_2O_3-TiO_2 Ceramic Materials, *J. Mater. Sci.*, 2007, **42**, p 9331-9335